Precision Adaptive Control Method for Automatic Switching Device of Power Grid Standby Power Supply

Cai-yun Di[1,2](✉)

[1] State Grid Jibei Electric Power Company Limited Skills Training Center, Baoding 071051, China
zz20221145@yeah.net
[2] Baoding Technical College of Electric Power, Baoding 071051, China

Abstract. In order to improve the effect of power grid standby power supply automatic switching device precision adaptive control, design a power grid standby power supply automatic switching device precision adaptive control method. Firstly, the inverter is modeled, then the instantaneous power is calculated when the standby power is switched automatically, and the mathematical model of doubly-fed induction generator is established. The experimental results show that the proposed control method can ensure the stability of power supply and voltage after control.

Keywords: Power grid · Standby power supply · Automatic switching device · Precision · Adaptive control · Voltage

1 Introduction

With the development of smart grid, the demand for power supply quality and reliability is becoming higher and higher. In particular, some customers have high demand for electricity, strict production processes and high level of automation. A sudden outage, even if it lasts only a few minutes, can shut down the entire production line, while resuming production takes a long time and is complex to operate. A sudden blackout will also bring a lot of economic losses to enterprises. People's lives have a tremendous impact, so that the national economy suffers huge losses.

The automatic standby power supply device is an important measure to ensure the continuity of power supply and improve the reliability of power supply. Using this device can simplify the configuration of power grid wiring and relay protection device to save equipment investment, reduce operational losses, and it has the advantages of simple structure, low cost, wide application, so it is widely used in power systems.

However, these devices can not meet the requirements of substation automation and unmanned shift, so a precision adaptive control method is designed for the standby power supply automatic switching device. Firstly, the inverter model is constructed, and

S. Liu and X. Ma (Eds.): ADHIP 2021, LNICST 417, pp. 270–283, 2022.
https://doi.org/10.1007/978-3-030-94554-1_22

then the instantaneous power during the automatic switching of standby power supply is calculated. Based on this, the mathematical model of doubly fed asynchronous generator is constructed to realize the droop control and adaptive state tracking control of the automatic switching device of power grid standby power supply. Finally, the accuracy and effectiveness of the adaptive control method are verified by simulation experiments.

2 Calculation Model of Instantaneous Power During Automatic Switching of Standby Power Supply

2.1 Inverter Modeling

The grid system consists of a number of inverter-based distributed generation units that rely on micropower sources for energy, such as fuel cells, micro gas turbines, DC storage, etc., while voltage source inverters are commonly used interface modules [1–3].

Specifically, the power distribution controller generates the amplitude and frequency of the inverter output voltage according to the droop characteristics. The voltage controller simulates the current vector of the reference filter inductance of a conventional synchronous generator, and the current controller synthesizes the instruction voltage vector by a pulse width modulation module. The voltage and current control loop must be able to provide sufficient damping to the filter composed of the filter and the coupled inductor. The coupling inductance determines the output impedance of the inverter, thus minimizing the coupling between active and reactive power [4]. Since the inverter of the micropower supply is controlled by a pulse signal, there is only one and only one upper or lower bridge arm on the same bridge arm, and they are alternately on each other, their switching function S_n can be defined, as shown in the formula below:

$$\begin{cases} S_n = 1 \quad (n = a, b, c) \\ S_n = -1 \ (n = a, b, c) \end{cases} \tag{1}$$

In formula (1), n represents the conduction parameter.

The midpoint of the DC bus filter capacitor is the reference point of the system shown, so the inverter bridge output phase voltage of the three-phase inverter can be indicated by the following formula:

$$\begin{bmatrix} V_a \\ V_b \\ V_c \end{bmatrix} = \begin{bmatrix} S_a \\ S_b \\ S_c \end{bmatrix} \cdot \frac{U_{dc}}{2} \tag{2}$$

Let the phase voltage of three-phase filter capacitor C_f and the current of three-phase filter inductor L_f be the state variables of the system. According to Kirchhoff's voltage and current law, the voltage and current equations are established for the phase voltage of three-phase filter capacitor C_f and three-phase filter inductor L_f respectively.

$$\begin{cases} C_f \frac{d}{dt} V_{oa} = i_a - i_{oa} \\ C_f \frac{d}{dt} V_{ob} = i_b - i_{ob} \\ C_f \frac{d}{dt} V_{oc} = i_c - i_{oc} \\ L_f \frac{d}{dt} i_a = V_a - V_{oa} - R_f i_a \\ L_f \frac{d}{dt} i_b = V_b - V_{ob} - R_f i_b \\ L_f \frac{d}{dt} i_c = V_c - V_{oc} - R_f i_c \end{cases} \tag{3}$$

In the formula (3), V_a, V_b and V_c are the inverter bridge output voltage of the three-phase inverter; i_a, i_b and i_c are the current of the three-phase filter inductor L_f; V_{oa}, V_{ob} and V_{oc} are the phase voltage of the three-phase filter capacitor C_f; i_{oa}, i_{ob} and i_{oc} are the current of the three-phase load.

Convert the above formula to a state space matrix [5, 6], which is represented as:

$$\begin{bmatrix} \dot{V}_{oa} \\ \dot{V}_{ob} \\ \dot{V}_{oc} \\ \dot{i}_a \\ \dot{i}_b \\ \dot{i}_c \end{bmatrix} = A \cdot \begin{bmatrix} V_{oa} \\ V_{ob} \\ V_{oc} \\ i_a \\ i_b \\ i_c \end{bmatrix} + B \cdot \begin{bmatrix} V_a \\ V_b \\ V_c \\ i_{oa} \\ i_{ob} \\ i_{oc} \end{bmatrix} \tag{4}$$

Modeling the inverter based on the above process can provide a basis for the adaptive control of automatic standby power supply switching device.

2.2 Calculation of Instantaneous Power in Automatic Switching of Backup Power

Based on the different topological structure of substation, different automatic bus switching models can be intelligently identified and generated by acquiring the real-time state of power network. The main function is to determine the current mode of operation of the system and to decide which model to use. The system combines the network analysis and the running state of the switch to judge the running mode of the current system, so as to decide which automatic switching mode to adopt. Therefore, the operation mode of the system must be accurately judged to prevent the misoperation and rejection due to misjudgment [7].

In order to reduce the maintenance workload and error rate effectively, the automatic generation algorithm of backup automatic switching model is developed in the main monitoring station of power network.

The design of the output inductance parameters is the core of the instantaneous power calculation. Firstly, a parameter ε_L of the fundamental voltage drop of the inductance is introduced, which is defined as the percentage of the fundamental voltage drop on the inductance L and the rated phase voltage U_g of the grid system, namely:

$$\varepsilon_{\mathrm{L}} = \frac{U_{\mathrm{L}}}{U_{\mathrm{d}}} \times 100\% = \frac{\omega L I_{\mathrm{n}}}{U_{\mathrm{g}}} \times 100\% \tag{5}$$

In formula (5), ω is the angular frequency of the fundamental voltage of the power grid, and I_n is the rated output current of the power grid. Since the system rated voltage is certain, the capacity of the power grid determines the rated current.

The vector relationship between the output voltage, the grid voltage and the inductance voltage. When connected to the grid, the minimum and maximum effective values of the output voltage are as follows:

$$U_{\mathrm{Imin}} = U_g - U_L = (1 - \varepsilon_L)U_d \tag{6}$$

If an unplanned isolated island occurs and the power grid fails, there is no power exchange between the grid and the main grid, and the load is supplied separately at this time, then the effective output voltage of the converter under the isolated grid is:

$$U_I' = U_L + U_{pcc}' = \varepsilon_L U_g + U_{FCC}' \tag{7}$$

In practical engineering, the ripple current on inductor L also has certain requirements under the premise of satisfying the requirements of inductor fundamental wave voltage drop [8, 9].

When the duty cycle reaches 50%, the current ripple is greatest, so there are:

$$\Delta_{\max} = \frac{T}{2} \times \frac{\mathrm{d}i}{\mathrm{d}t} = \frac{TU_{dc}}{4L} = \frac{U_{\mathrm{dc}}}{4Lf_{\mathrm{sw}}} \tag{8}$$

From the above formula, the ripple current and the DC side voltage from the above formula, the ripple current and DC side voltage U_{dc}, inductance L and switching frequency f_{sw} are related. The DC side voltage is proportional to the ripple current, while the inductance is inversely proportional to the switching frequency.

Define a ripple coefficient parameter η_L, which is one half of the maximum peak ripple current as a percentage of the rated current I_n of the grid system, namely:

$$\eta_L = \frac{\Delta i_{\max}}{2I_n} \times 100\% \tag{9}$$

In order to apply the droop control strategy, the instantaneous active and reactive power output from the micropower interface must first be calculated, using the two-axis theory [10], the instantaneous active and reactive components p and q injected are expressed as follows:

$$\begin{aligned} p &= v_{od} i_{od} + v_{oq} i_{oq} \\ q &= v_{od} i_{oq} - v_{oq} i_{od} \end{aligned} \tag{10}$$

In order to have enough time span to separate power and current control loop and achieve high power quality injection, the average active power, reactive power and the corresponding fundamental component are affected by the control action. The instantaneous power component is used to obtain the active power p and reactive power Q related to the fundamental component through the lowpass filter shown in the following formula.

$$P = \frac{w_c}{s + w_c} p, Q = \frac{w_c}{s + w_c} q \tag{11}$$

In formula (11), w_c is the cut-off frequency of the filter.

3 Precision Adaptive Control of Automatic Switching Device for Standby Power Supply

3.1 Mathematical Model Construction of Doubly Fed Induction Generator

Double-fed asynchronous generator is a rising technical direction, mainly used in some large variable-speed wind turbine. In doubly fed asynchronous motors, a voltage-type transducer transmits power at differential frequencies to H-phase rotors, so the motor receives energy from both stator and rotor ends. The generator model introduced in this section ignores the hysteresis loss, eddy current loss and molten iron loss, and only considers the fundamental current component of stator and rotor, not the harmonics. The positive directions of the voltage, current and electromagnetic torque on the stator side of the motor are specified in accordance with the generators' practice; and the positive directions of the voltage, current and electromagnetic torque on the rotor side of the motor are specified in accordance with the electrification practice [11, 12]. According to the equivalent circuit diagram of the double-feed generator, the basic equations are as follows:

$$\begin{aligned} \dot{U}_1 &= -\dot{E}_1 - \dot{I}_1(R_1 + jX_1) \\ \frac{\dot{U}_2'}{s} &= -\dot{E}_2' + \dot{I}_2'\left(\frac{\dot{R}_2'}{s} + jX_1'\right) \\ \dot{E}_1 &= \dot{E}_2' = -\dot{I}_\mathrm{m}(R_m + jX_m) \\ \dot{I}_1 &= \dot{I}_2' - \dot{I}_\mathrm{m} \end{aligned} \tag{12}$$

In the formula (12), R_1 and X_1 are the equivalent resistance and equivalent reactance of the stator winding; $\dot{E}_1$, $\dot{U}_1$ and $\dot{I}_1$ are the induced electromotive force, voltage and current of the stator side winding respectively; $\dot{R}_2'$ and X_m are the equivalent resistance and equivalent reactance of the rotor winding respectively converted to the value of the stator side; $\dot{E}_1$ and $\dot{E}_2'$ are the value of the induced voltage and current of the rotor winding converted to the value of the stator side respectively; $\dot{U}_2'$ is the value of the voltage of the rotor side excitation source converted to the value of the stator side respectively; R_m is the excitation resistance.

Double-fed wind turbines are a multivariable, strongly dependent, hierarchical system. In order to simplify the analysis and calculation, it is generally assumed that:

1. Stator windings of H phase with symmetrical distribution and spatial difference of 120 degrees, which ignore the influence of harmonics and magnetic saturation, generate magnetokinetic potential with sinusoidal distribution along air gap [13–15];
2. H phase winding of the rotor is of symmetrical structure;
3. Ignoring the influence of temperature, ignoring the iron loss and the skin effect.

3.2 Sag Control

After the above foundation treatment, the sag is controlled. It can be seen from the basic concept and flexible structure of power grid that the variable operation mode of power grid and the power supply service of high power quality depend on its perfect control system.

Master-Slave Control and Master-Slave Control are the control methods based on control strategy for isolated island power network. The reference voltage and frequency are provided by one or a limited number of micro-power sources, which can support the voltage and frequency of the power grid system [16]. At present, the master-slave control strategy still has some disadvantages: the fluctuation of load is balanced by the master power, so the master power is required to have certain capacity; the slave power is controlled by the master power, so the master power is too dependent on the master power; the master-slave control relies on communication, so it is restricted by the cost, complexity and reliability of communication.

Peer to Peer control, Peer to Peer control, means that there is no subordinate relationship between distributed generation and a distributed generation in the system use droop control method to regulate active and reactive power. At present, the problems of the equivalent control method are: the steady-state error can not be zero because of the instantaneous change of load; the harmonic distribution caused by non-linear load can not be coordinated; the droop characteristic method can not solve the problem that the reactive power of the system is affected by the line impedance; for the system with linear and non-linear load, the equivalent control method will not be applicable when the control mode changes due to the change of topology structure [17].

Multi-agent technology, with the rapid development of artificial intelligence, multi-agent system has been widely used. Multi-agent technology is suitable for decentralized and complex control of power network. Therefore, it can be applied to power system reconfiguration, power supply restoration, power market transaction and energy optimization and intelligent management. But at present, the application of multi-agent technology in power grid is mainly focused on the coordination of market transactions, power supply recovery and energy management, etc. In order to make multi-agent technology play a greater role in power system control systems, there is still a lot of research work to be done.

In order to ensure the normal operation of different kinds of micro-power supply, the power control method of the inverter interface of micro-power supply will use similar parallel power control method, even using similar method to the droop control of synchronous generator. This control method has the following advantages:

The micro-power supply in the power grid can be installed in any position, and will not be disturbed by some uncontrollable factors [18].

In the case of active power and reactive power balance of power grid, any micro-power supply can be integrated into or separated from the power grid, and this will not have a great impact on the power grid system.

When any micropower supply in the grid fails, the grid system can maintain the faulty micropower supply without stopping operation, and can guarantee the uninterrupted and reliable power supply to the grid load.

When the communication fault occurs between the micropower control unit and the central control unit of the power grid, the power grid system can still operate normally to ensure the reliability of the system.

Different from the traditional sag control method applied to synchronous generators, it is difficult to apply the sag control method to micro-power inverter. The self-characteristic of synchronous generator accords well with the droop characteristic, that is, when the input power of the prime mover is invariable, the increase or decrease of the load will make the speed of synchronous generator decrease or increase automatically to achieve balance. Unlike synchronous generators, micropower inverters cannot be balanced by regulating the generation of micropower, but rely on their own control strategies to achieve this balance [19, 20] (Fig. 1).

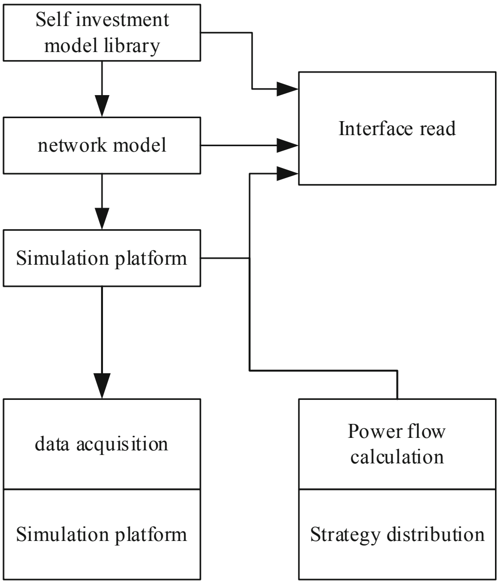

Fig. 1. Sagging control content

To sum up, the active power output of micropower can be regulated by controlling the output frequency, and the reactive power output can be regulated by controlling the output voltage amplitude of micropower [21]. Therefore, some researchers proposed using the droop control method to control the micro-power inverter. In order to realize the power distribution function in the parallel inverter system, the traditional droop control characteristics are introduced. The droop characteristics based on voltage frequency and output voltage amplitude are shown as follows:

$$w = w^* - mP \tag{13}$$

$$V = V^* - nQ \tag{14}$$

In the formulae (13) and (14), w^* and V^* shall be the rated frequency and voltage setting points; m and n shall be the static sag gain.

Under the sag control strategy, the active and reactive power output of the inverter unit is detected, then the rated frequency and voltage are obtained, and finally the active and reactive power output is reversely adjusted.

It can be seen from the sag characteristics that when the active power of the micropower output is larger, the output active power of the micropower output can be reduced by reducing the output frequency, whereas, when the active power of the micropower output is smaller, the output active power of the micropower output can be improved by increasing the output frequency; when the reactive power of the micropower output is larger, the output reactive power of the micropower can be reduced by reducing the output voltage amplitude, and vice versa, the output reactive power of the micropower output can be improved by increasing the output voltage amplitude. Through the adjustment of the above droop control strategy, the micropower in the power grid can realize the reasonable distribution of its active and reactive power.

3.3 Adaptive State Tracking Control Implementation

Before the 1960s, adaptive control was mainly used in aviation and space applications. Adaptive control focuses on the attitude control of aircraft, and many kinds of flight control schemes are proposed and realized. After the mid-1960s, adaptive control began to be gradually extended to the field of industrial control. Since the 1970s, adaptive control has been widely used in many fields. Now, adaptive control has been used in various fields maturely. The most commonly used definition of adaptive control is that an adaptive control system is one in which, when operating conditions are uncertain or change over time, it is able, during the control period, to implement effective controls based on information accumulated from online observations of reachable inputs and outputs, and to modify the parameters and control effects of the system structure so that the system is in a prescribed (and generally near-optimal) state.

Based on the idea of self- adaptive control, it is applied to the automatic switching device control of standby power supply. Uncertainties exist widely in practical control systems, and switched systems are no exception. Adaptive control is an effective method to deal with uncertain parameters, because the parameters of control are adjusted continuously according to control effect or on-line identification. Adaptive control of switched systems is a new research direction in five years, which has attracted more and more attention from the academic circles at home and abroad. With the development of research, the research on adaptive control of linear switched systems has gained some results. Consider nonlinear switched systems [22]:

$$\dot{x} = f_{\sigma 1}(x) + \theta_{\sigma 1} f_{\sigma 2}(x) + B_{\sigma} u \tag{15}$$

In formula (15), $f_{\sigma 1}(x)$ represents the state vector of the system, $\theta_{\sigma 1}$ is the matrix of unknown constants, $B_{\sigma} u$ is the matrix of known inputs, and $f_{\sigma 2}(x)$ is a known continuous function. The control objective of this paper is to design switching signals for switching systems, and to design adaptive controllers and adaptive laws for all subsystems so that the signals of closed-loop systems are bounded while $\lim_{t \to \infty} x(t) = 0$.

Considering that all subsystems can not be stabilized by designing state feedback adaptive controller, it is necessary to keep the stabilizable subsystem active all the time to achieve the goal of control. For each $i \in \Lambda$, the matrix K_{i1}^{*} satisfies [23, 24]:

$$\frac{\partial V_i}{\partial x}\big(f_i(x) + B_i K_{i1}^{*} \Phi_i(x)\big) + \sum_{j \neq 1} \beta_{ij}(x)\big(V_j(x) - V_1(x)\big) < 0 \tag{16}$$

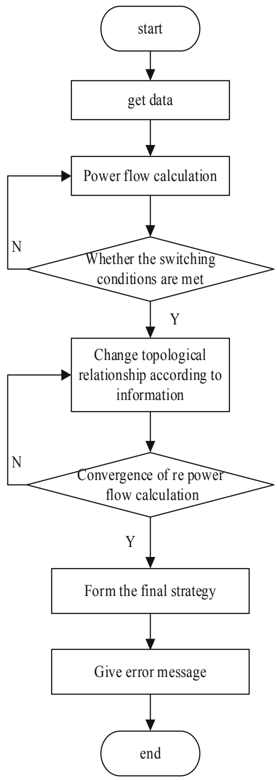

Fig. 2. Control the algorithm process

In the formula (16), $V_j(x)$ is positively definite and radially unbounded (Fig. 2).

The hyperstability theory is rooted in the theory of dissipation and passivity, which states that if the system is passive (strictly passive) with a finite input of external energy, the state of the system itself is bounded (bounded and convergent). The adaptive system can be regarded as the feedback interconnection structure of the control error system and the adaptive controller. In the design process, the hyperstability theory is applied to the system. In other words, the controller structure is chosen to make the control error system passive, and the adaptive law is chosen to ensure that the energy of the control error system is limited.

The basic idea is that the boundedness and convergence of the state are obtained by the boundedness and convergence of the energy of the system in the study of the traditional non-switched systems. This section focuses on a single subsystem to consider the problem, by studying the energy changes of the subsystem to obtain the hyperstability of the switching system. For each subsystem, the energy storage function is affected by the external energy input during the activation period, and the energy change is restricted by the state evolution of other subsystems during the non-activation period. Connecting the activation and non-activation periods, we can get the energy change of the subsystem in the continuous time domain, so we can study the properties of the system from the energy point of view. Consider linear switching systems:

$$\begin{aligned} \dot{x} &= A_\sigma x + B_\sigma u \\ y &= C_\sigma x + D_\sigma u \end{aligned} \tag{17}$$

In formula (17), $A_\sigma x$ is the output of the system, $C_\sigma x$ is the input of the system, $B_\sigma u$ is the state matrix, and Q is the input matrix.

Let $V_i(x)$ be the energy storage function of the i subsystem. If the switched system is dissipative, it has:

$$V_i(x(t)) - V_i(x(s)) \leq \int_s^t \omega_i^i(u(\tau), y(\tau))d\tau \tag{18}$$

In the formula (18), $V_i(x(s))$ represents the self-energy supply rate when the i subsystem is activated, and $d\tau$ represents the interactive supply rate.

Based on the above process, the adaptive control of power supply automatic switching device precision is completed.

4 Simulation Experiment

In order to verify the validity of the precision adaptive control method of the standby power supply automatic switching device, the experiment was carried out and compared with the traditional control method. The simulation parameters applied in this experiment are shown in Table 1:

Table 1. Experimental parameters

Serial number	Parameter	Value
1	Active power capacity of power grid	20 kW
2	Rated voltage of power grid	220 V
3	Grid voltage angle frequency	50 × 2π rad/s
4	DC side voltage	700 V
5	Switching frequency	10 kHz

4.1 Comparison of Voltage Stability After Control

The fastest single opening and closing time of the power grid standby power supply automatic switching device is 225 ms, and the device is used in the substation, with large working current and arc extinguishing time of more than 65 ms. In addition, judging the loss of voltage by detecting AC, the "standby automatic switching" can complete the power supply switching within 512 ms at the fastest; By optimizing the device structure and changing the application scenario, the single bounce time of solid-state permanent magnet structure is 20 ms, the arc extinguishing time is 8 ms, the calculated DC zero crossing time is 6 ms, and the starting and closing time is 20 ms. The proposed method is compared with the traditional method. The results of voltage stability comparison between the proposed method and the traditional method are shown in Fig. 3.

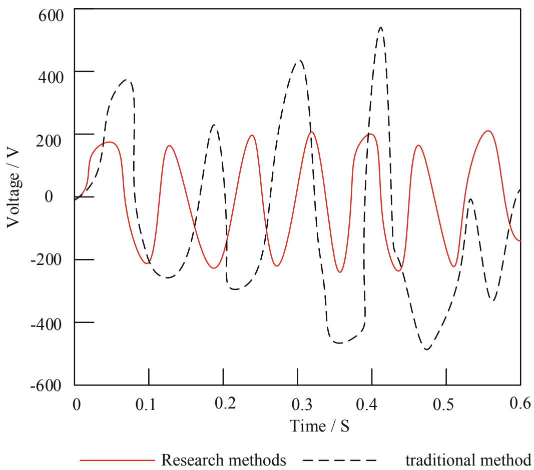

Fig. 3. Comparison of voltage stability after control

It can be seen from the analysis of Fig. 3 that the voltage stability of the adaptive control method in this study is better, and the overall value is more stable, while the voltage stability of the traditional method is obviously poor, and the fluctuation is more obvious.

4.2 Current Comparison After Control

The current comparison results of the two methods are shown in Fig. 4.

Based on Fig. 4, it can be seen that after the control of this research method, the current value is relatively stable, which can make a smooth transition and meet the good power supply quality of the load, which is more stable than the traditional method. It can be proved that the control effect of the adaptive control method is good.

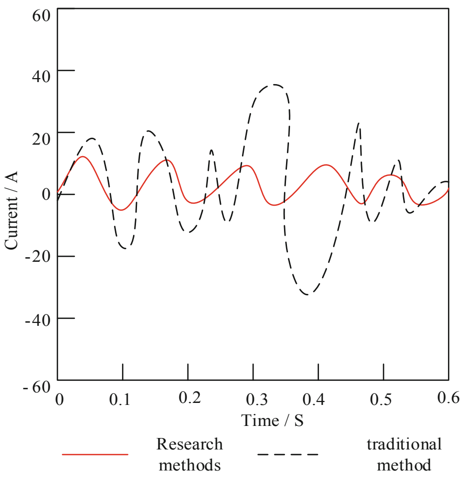

Fig. 4. Control the rear current comparison

5 Conclusion

With the acceleration of the construction of "one strong and three excellent", it is the responsibility of power grid enterprises to continuously improve the power supply reliability of power grid. Reasonable power grid structure and operation mode are the basis to ensure the safe and stable operation of power system. Whether relay protection devices can play an effective role is closely related to the power grid structure and operation mode, which must be considered as a whole. Therefore, according to the actual situation of power grid, the precision adaptive control method of automatic switching device of power grid standby power supply is designed, which is a powerful guarantee to improve the reliability of power supply.

With the development of smart grid technology, a large number of energy storage and distributed generation will be connected to the distribution network; In case of "N-1" fault under equipment maintenance mode, the power transfer mode between lines will be more flexible after the standby automatic switching action. How to establish the optimal configuration model of standby automatic switching for intelligent distribution network compatible with distributed generation and energy storage is the focus of the next step.

References

1. Zou, Z.X., Buticchi, G., Liserre, M.: Grid identification and adaptive voltage control in a smart transformer-fed grid. IEEE Trans. Power Electron. **34**(3), 2327–2338 (2019)
2. Jalalabadi, E., Salehizadeh, M.R., Kian, A.R.: Optimal control of the power ramp rate with flicker mitigation for directly grid connected wind turbines. Simulation **96**(2), 141–150 (2020)
3. Zhang, Y., Wei, W.: Decentralised coordination control strategy of the PV generator, storage battery and hydrogen production unit in islanded AC microgrid. IET Renew. Power Gener. **14**(6), 1053–1062 (2020)

4. Qian, Q., Xie, S., Xu, J., Bian, S., Zhong, N.: Passivity-based output admittance shaping of the converter-side current-controlled grid-tied inverter to improve the robustness to the grid impedance. IET Power Electron. **13**(10), 1956–1965 (2020)
5. Chen, X., Wang, X., Jian, J., Tan, Z., Li, Y., Crossley, P.: Novel islanding detection method for inverter-based distributed generators based on adaptive reactive power control. J. Eng. **2019**(17), 3890–3894 (2019)
6. Mondal, P., Tripathy, P., Adda, R., Saha, U.K.: Development of an adaptive control strategy for the three-phase grid side converter with wide range of parametric and load uncertainties. IET Power Electron. **13**(12), 2399–2412 (2020)
7. Giri, A.K., Arya, S.R., Maurya, R., Chittibabu, B.: Control of VSC for enhancement of power quality in off-grid distributed power generation. IET Renew. Power Gener. **14**(5), 771–778 (2020)
8. Ancha, S.K., Padhy, B.: Adaptive droop control strategy for autonomous power sharing and DC voltage control in wind farm-MTDC grids. IET Renew. Power Gener. **13**(16), 3180–3190 (2019)
9. Shukl, P., Singh, B.: Grid integration of three-phase single-stage PV system using adaptive laguerre filter based control algorithm under nonideal distribution system. IEEE Trans. Ind. Appl. **55**(6), 6193–6202 (2019)
10. Liu, S., Liu, D., Srivastava, G., Połap, D., Woźniak, M.: Overview and methods of correlation filter algorithms in object tracking. Compl. Intell. Syst. **7**(4), 1895–1917 (2020)
11. Abdulrahman, I., Belkacemi, R., Radman, G.: Power oscillations damping using wide-area-based solar plant considering adaptive time-delay compensation. Energy Syst. **12**(2), 459–489 (2019)
12. Liu, S., Liu, X., Wang, S., Muhammad, K.: Fuzzy-aided solution for out-of-view challenge in visual tracking under IoT assisted complex environment. Neural Comput. Appl. **33**(4), 1055–1065 (2021)
13. Li, Z., et al.: Adaptive power point tracking control of PV system for primary frequency regulation of AC microgrid with high PV integration. IEEE Trans. Power Syst. **36**(4), 3129–3141 (2021)
14. Gupta, Y., Chatterjee, K., Doolla, S.: A simple control scheme for improving reactive power sharing in islanded microgrid. IEEE Trans. Power Syst. **35**(4), 3158–3169 (2020)
15. Santhoshi, B.K., Mohanasundaram, K., Kumar, L.A.: Ann-based dynamic control and energy management of inverter and battery in a grid-tied hybrid renewable power system fed through switched z-source converter. Electr. Eng. **103**(5), 2285–2301 (2021)
16. Zhao, B.Y., Zhao, Z.G., Li, Y., Wang, R.Z., Taylor, R.A.: An adaptive PID control method to improve the power tracking performance of solar photovoltaic air-conditioning systems. Renew. Sustain. Energy Rev. **113**, 109250 (2019)
17. Liu, Z., Miao, S., Fan, Z., Liu, J., Tu, Q.: Improved power flow control strategy of the hybrid AC/DC microgrid based on VSM. IET Gener. Transm. Distrib. **13**(1), 81–91 (2019)
18. Pandey, S.K., Singh, B., Modi, G.: Frequency adaptive complex coefficient filter based control for grid integrated PV system. IET Generat. Transm. Distrib. **14**(19), 4141–4151 (2020)
19. Offringa, A.R., Mertens, F., Van, D., Veenboer, B., Gehlot, B.K., Koopmans, L., et al.: Precision requirements for interferometric gridding in 21-cm power spectrum analysis. Astron. Astrophys. **631**, A12 (2019)
20. Gong, P., Lu, Z., Lin, J., Lv, Z.: Distributed secondary control based on cluster consensus of inhibitory coupling with power limit for isolated multi-microgrid. IET Gener. Transm. Distrib. **13**(18), 4114–4122 (2019)
21. Shah, P., Singh, B.: Adaptive observer based control for roof-top solar PV system. IEEE Trans. Power Electron. **35**(9), 9402–9415 (2019)

22. Hu, C., He, H., Jiang, H.: Edge-based adaptive distributed method for synchronization of intermittently coupled spatiotemporal networks. In: IEEE Transactions on Automatic Control, pp. 1–1 (2021)
23. Nguyen, A.T., Lee, D.C.: Sensorless control of DFIG wind turbine systems based on SOGI and rotor position correction. IEEE Trans. Power Electron. **36**(5), 5486–5495 (2021)
24. Yin, Y., Vazquez, S., Alcaide, A.M., Liu, J., Franquelo, L.G.: Observer-based sliding mode control for grid-connected power converters under unbalanced grid conditions. In: IEEE Transactions on Industrial Electronics, pp. 1–1 (2021)